An Enhanced Aquila Optimizer Algorithm for Resource Allocation in Indoor Multi-user IoT VLC System

Selma Yahia[1], Yassine Meraihi[1], Sylia Mekhmoukh Taleb[1], Seyedali Mirjalili[2], Amar Ramdane-Cherif[3], Tu Dac Ho[4], Hossien B. Eldeeb[5], and Sami Muhaidat[5]
[1]LIST Laboratory, University of M'Hamed Bougara Boumerdes, Avenue of Independence, Boumerdes, Algeria.
[2]Centre for Artificial Intelligence Research and Optimisation, Torrens University Australia, Brisbane, Australia.
[3]LISV Laboratory, University of Versailles St-Quentin-en-Yvelines, 10-12 Avenue of Europe, Velizy, France.
[4]Department of Electrical Engineering, Faculty of Engineering Science and Technology, UiT, Arctic University of Norway.
[5]Center of Cyber-Physical Systems, Electrical Engineering Computer Science, Khalifa University, UAE.
E-mail: s.yahia@univ-boumerdes.dz

***Abstract*—Visible light communication (VLC) is a rapidly growing wireless communication technology for the Internet of Things (IoT) that offers high data rates and low latency, making it ideal for massive connectivity. Efficient resource allocation is essential in VLC networks to minimize inter-symbol and co-channel interferences, which can greatly improve network performance and user satisfaction. This paper focuses on an indoor IoT-based VLC system that utilizes photodetectors (PDs) on users' cell phones as receivers, with the goal of maximizing system performances and reducing power consumption by selectively activating some PDs while deactivating others. However, this objective presents a challenge due to the inherent non-convex nature of the multi-objective optimization problem, which cannot be solved by analytical means. To address this, we propose an enhanced Aquila optimization (EAO) scheme that improves upon the Aquila Optimizer (AO) by incorporating a fitness distance balance (FDB) function. We evaluate our proposed EAO in various scenarios under different settings, considering both capacity and fairness metrics. Through simulations, we demonstrate the effectiveness of our approach and its superiority over classical algorithms such as Aquila Optimizer (AO), Particle Swarm Optimization (PSO), and Grey Wolf Optimization (GWO) in finding the optimal solution. Our results confirm that the proposed EAO algorithm can efficiently optimize the system capacity and ensure fairness among all users, providing a promising solution for indoor VLC systems.**

***Index Terms*—Aquila Optimizer, Enhanced Aquila Optimizer, Visible Light Communications, Resource Allocation.**

I. Introduction

Internet of Things (IoT) is a burgeoning technology that has tremendous potential to reshape society and revolutionize industries [1]. By enabling the interconnection of physical objects, IoT has the power to drive transformative advancements in areas such as indoor, smart manufacturing, smart grids, and smart cities, among others [2]. However, the current wireless access networks for IoT rely primarily on radio frequency (RF) communication technologies. RF suffers from significant limitations, including overcrowded spectrum and limited bandwidth, which can impede the extensive connectivity demands of IoT networks [3]. To address these challenges, visible light communication (VLC) is emerging as a promising complementary technology to RF communication. VLC leverages the visible light spectrum for high-speed data transmission, lower latency, and a larger available spectrum [4]. By integrating VLC into IoT networks, the limitations of RF can be overcome, enabling the development of more efficient, reliable, and scalable IoT systems [5].

VLC utilizes light-emitting diodes (LEDs) as wireless transmitters, taking advantage of their dual functionality as lighting devices and access points (APs) for internet and wireless connectivity [6]. However, IoT-VLC systems face performance degradation issues, such as limited LED coverage due to the need for a clear direct communication link connecting the transmitter and the receiver. To address this challenge, the authors in [7] deployed multiple access points to serve multi-users (MU) within designated lighting zones. However, multipath reflections can still introduce inter-symbol interference (ISI), which negatively impacts MU-IoT-VLC network performance. Therefore, resource allocation schemes are necessary to minimize interference and optimize system performance [8].

Optimizing resource allocation in VLC systems is crucial for achieving maximum performance. However, few attempts have been made to address this issue in indoor IoT-VLC systems. For instance, in [9], a resource allocation issue is addressed in the context of indoor positioning multi-cell systems. The objective of their proposal is to maximize the overall sum rate while meeting device positioning accuracy requirements. Similarly, in [10], the authors addressed a dynamic resource allocation problem in an indoor IoT-VLC system. Their approach focuses on maximizing the overall user throughput while reducing the user packet loss rate. In [11], an optimal fair resource allocation strategy based on Genetic Algorithm (GA) was developed in indoor uplink VLC system to enhance the signal-to-interference-plus-noise ratio (SINR) and fairness of users. The notion of fairness represents the measures used to assess and ensure equitable distribution of system resources among users or applications. In [12], the

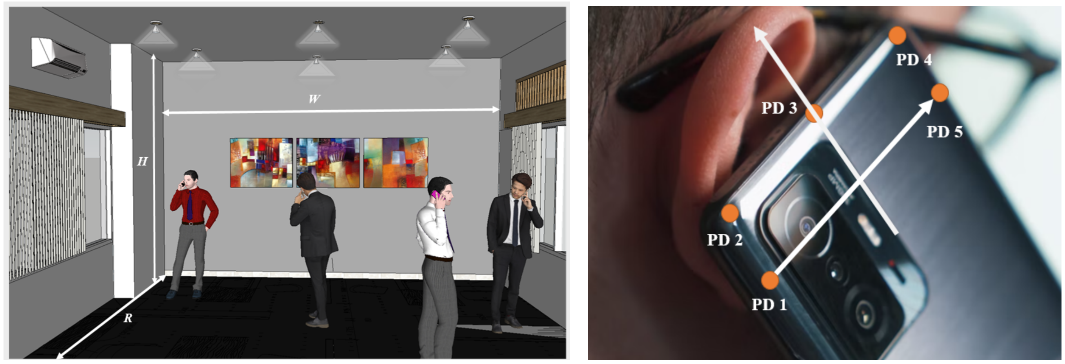

(a) (b)

Fig. 1: (a) The considered scenario (b) Location of PDs on the user's cell phone.

authors introduce an optimization problem that focuses on minimizing the overall energy consumption of multiple LEDs while ensuring the fulfillment of quality of service (QoS) criteria.

It is important to highlight that the aforementioned studies [9]–[12] have limitations in terms of supporting a large number of users (e.g., the work in [11] was limited to less than 10 users) and ensuring fairness between users, which are vital for practical deployments. For instance, optimizing only the maximum capacity can lead to performance degradation and even disconnection for users located at the edge of the coverage area. Therefore, in this paper, we develop a joint optimization problem that aims to enhance the overall system capacity and ensure fairness among all users while minimizing the power consumption at the receiver side.

In this paper, we focus on an indoor IoT-based VLC system that serves multiple users, with each user having multiple photodetectors (PDs) installed on their mobile phones to receive signals. To optimize system performance and minimize power consumption, we select a subset of PDs to be turned on while the others remain off. To achieve this, we develop a joint optimization problem that enhances overall system capacity and ensures fairness among all users. To solve this non-convex multi-objective optimization problem, we propose an advanced optimization method called Enhanced Aquila Optimizer (EAO), which builds upon the Aquila optimizer (AO) algorithm and integrates a Fitness Distance Balance (FDB) function to improve its performance and accuracy.

The paper is structured as follows. In Section II, we present the system model and formulate the resource allocation problem. Section III discusses the AO and FDB strategy. In Section IV, we explain the proposed EAO framework for solving the resource allocation problem. In Section V, numerical results are presented, and a comparative analysis of the proposed EAO approach against other algorithms in the literature is conducted. Finally, Section VI concludes the paper.

II. System Model and Scenarios

A. Scenarios Under Consideration

In Fig. 1, we present our indoor IoT-VLC system that serves multiple users (nodes) in a room with dimensions $R \times W \times H$ (as depicted in Fig. 1a). The ceiling of the room is equipped with L LEDs that act as optical transmitters for IoT communication. The LEDs are uniformly distributed for consistent coverage and emit the same messages to all users with a fixed optical power of P_t. The system caters to multiple users N who are equipped with M PDs, each with an aperture diameter of D_r and a responsivity of ρ. These PDs are evenly distributed on each user's cell phone (as shown in Fig. 1b). We examine the distribution of users in three different scenarios as follows.

- **Scenario 1:** In this scenario, N_1 users are assumed to be stationary in fixed positions within the room (see Fig. 2a). On other words, the users' positions remain unchanged throughout the analysis.
- **Scenario 2:** In this scenario, N_2 users are assumed to be in motion, following different trajectory directions, randomly generated, (see Fig. 2b). The scenario unfolds as follows:
  - At time t: The users are initially positioned at Sc1.
  - At time t+1: The users move from their initial positions in Sc1 to different positions described by Sc2.
  - At time t+2: The users move once again to Sc3.
- **Scenario 3:** In this scenario, N_3 users are randomly distributed within the room (see Fig. 2c). The positions of the users are randomly assigned, creating a varied distribution throughout the room. The average performance is then considered in our analysis.

For channel modeling, we adopt the reference IEEE channel models [13], which is based on non-sequential ray tracing methodology of OpticStudio® software. This approach enables the modeling of light propagation through the environment in a flexible and realistic manner, taking into account diffusion and reflection at any object encountered. The detailed steps of this methodology can be found in [14].

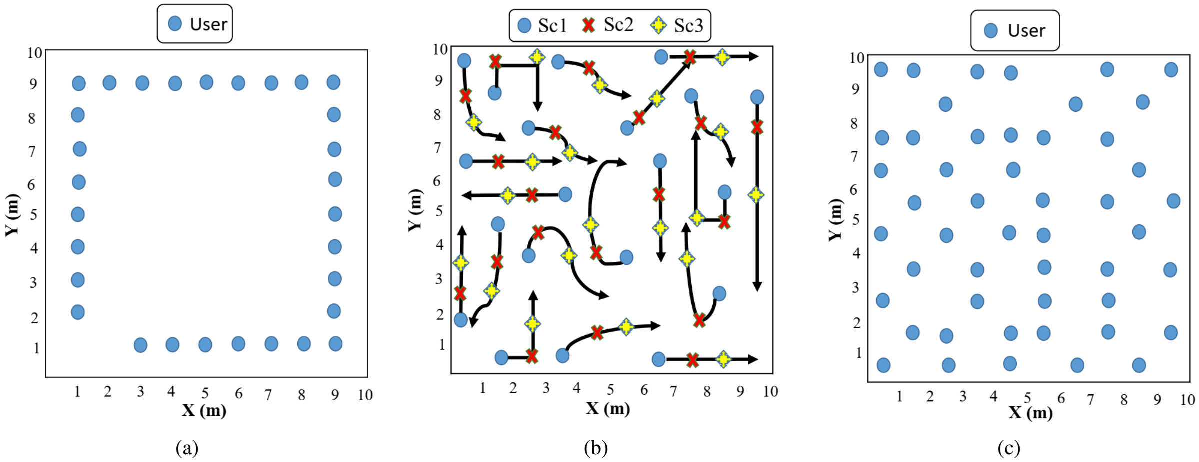

Fig. 2: (a) Scenario 1 (b) Scenario 2 (c) Scenario 3

B. Problem Definition and Performance Metrics

The problem we aim to solve involves an indoor IoT-VLC system that caters to multiple users, each equipped with several PDs. To conserve energy and prolong the life of the devices, we only activate the optimal PD while turning off the others. However, we need to allocate operational PDs among different users to improve the network's overall performance in terms of total capacity and user's fairness while satisfying a reliable communication. To achieve this goal, we use an assignment matrix A $(N \times M)$ that summarizes the activation and deactivation states of all PDs associated with different users and is given by

$$A = \begin{pmatrix} S_{11} & S_{12} & \cdots & S_{1M} \\ S_{21} & S_{22} & \cdots & S_{2M} \\ \vdots & \ddots & \vdots & \vdots \\ S_{N1} & S_{N2} & \cdots & S_{NM} \end{pmatrix}, \tag{1}$$

where S_{lk} is a binary allocation variable associated with the k^{th} PD of the l^{th} user. This variable takes a value of 1 in case of the PD is selected to be active and 0 otherwise, as only one PD can be active at any given time t. Therefore, the sum of all allocation variables corresponding to user l must be equal to one, i.e., $\left(\sum_{k=1}^{M} S_{lk} = 1\right), \forall l \in \{1, 2, \cdots, N\}$. We also introduce a vector $\bar{S}$ to indicate the active PD's indexes of all users. This vector is denoted as $\bar{S} = [S_1', S_2', ..., S_N']$, thus $S_l' \in \{1, 2, \ldots, M\}$ indicates the active PD's index related to the l^{th} user. Accordingly, we can express the values of the binary variables S_{lk} as [11]:

$$S_{lk} = \begin{cases} 1, & k = S_l' \\ 0, & \text{otherwise} \end{cases}. \tag{2}$$

The SINR at the k^{th} PD of the l^{th} user can be expressed as follows [15] :

$$\gamma_{lk} = \frac{\rho^2 \left(P_t H_{lk} S_{lk}\right)^2}{\sigma_0^2 + \sigma_{I_{lk}}^2}, \tag{3}$$

where H_{lk} represents the channel gain at the k^{th} PD of the l^{th} user, determined through the ray tracing technique outlined in [13] and the toolbox available in [16]. Also, the total noise variance σ_0^2 is defined as $\sigma_0^2 = N_0 B$, where N_0 represents the spectral density of the noise power and B denotes the bandwidth. In (3), $\sigma_{I_{lk}}^2$ denotes for the ISI coming from reflections. In downlink VLC systems with data rates of few Mb/s and single carrier with simple modulation schemes (, i.e., PAM), the impact of $\sigma_{I_{lk}}^2$ can be neglected since the assumption of frequency flat channel can be considered. Based on (3) and under the assumption of $\mathcal{Q}$-ary PAM modulation scheme, the error rate at the k^{th} PD of the l^{th} user ($P_{e_{lk}}$) is calculated by [17]

$$P_{e_{lk}} = \frac{(\mathcal{Q}-1)}{\mathcal{Q}\log_2(\mathcal{Q})} \operatorname{erfc}\left(\sqrt{\frac{3}{2(\mathcal{Q}-1)(2\mathcal{Q}-1)}\gamma_{lk}}\right), \tag{4}$$

where $\mathcal{Q}$ and $\operatorname{erfc}(\cdot)$ are the modulation size and the complementary error function, respectively. The corresponding user capacity is also given by [18]

$$C_{lk} \approx \frac{B}{2\ln(2)} \ln\left(1 + \frac{\exp(1)\gamma_{lk}}{2\pi}\right). \tag{5}$$

The total achievable capacity for an allocation vector $S_{lk} = \bar{S}$ can be then defined as the sum of individual capacities of all users given as $C_T(\bar{S}) = \left(\sum_{l=1}^{N} C_{lk}(\bar{S})\right)$. Furthermore, the Jain fairness index, which measures the degree of fairness in allocating the PDs among the users, associated with the allocation vector $S_{lk} = \bar{S}$ can be calculated by [11], [19]:

$$F(\bar{S}) = \frac{\left(\sum_{l=1}^{N} C_{lk}(\bar{S})\right)^2}{N\sum_{l=1}^{N}\left(C_{lk}(\bar{S})\right)^2}. \tag{6}$$

C. Problem Formulation

To formulate the optimization problem under consideration, the objective function should first reflect the two objectives of our indoor IoT VLC system: ***i***) Maximizing the total capacity and ***ii***) Maximizing the fairness of each user. Then, we need to ensure the following constraints: **a) Error rate constraint:** To achieve reliable communication for each user, the error-rate must be below a certain threshold, denoted as $P_{e_{\text{th}}}$. **b) Activation constraint:** Only one PD should be active for each user at any given time, which can be expressed as: $\sum_{k=1}^{M} S_{lk} = 1, \forall l \in \{1, 2, ..., N\}$. **c) Fairness constraint:** All users should satisfy the minimum desired fairness level (F_{min}), i.e., $F(S_{lk}) \geq F_{min}$. **d) Non-negativity constraint:** We impose an additional constraint that reflects the practical limitations of the system, i.e., $S_{lk} \geq 0$, for all $l \in \{1, 2, ..., N\}$ and $k \in \{1, 2, ..., M\}$. Therefore, to achieve this, we use a weighted sum of two objective functions where two weights are utilized to reflect the relative importance of each objective, i.e., w_1 and w_2 are the weights assigned to the capacity and fairness objectives, respectively. Our multi-objective problem can be finally expressed as follows.

$$\max_{S_{lk}} \quad w_1 \sum_{l=1}^{N} \sum_{k=1}^{M} S_{lk} C_{lk} + w_2 F(S_{lk}) \tag{7}$$

s.t

$$\textbf{C1}: \; P_{e_l}(S_{lk}) \leq P_{e_{\text{th}}}, \quad \forall l \in \{1, 2, \cdots, N\} \tag{8a}$$

$$\textbf{C2}: \quad \sum_{k-1}^{M} S_{lk} = 1, \quad \forall l \in \{1, 2, \cdots, N\} \tag{8b}$$

$$\textbf{C3}: \; F(S_{lk}) \geq F_{min}, \; \forall l \in \{1, 2, \cdots, N\} \tag{8c}$$

$$\begin{aligned} \textbf{C4}: \quad S_{lk} \geq 0, \quad & \forall l \in \{1, 2, \cdots, N\} \quad \& \\ & \forall k \in \{1, 2, \cdots, M\} \end{aligned} \tag{8d}$$

The above multi-objectives optimization problem under consideration is a non-convex one. Non-convex optimization problems are difficult to solve analytically, and specialized optimization techniques, such as heuristic algorithms can be used. Therefore, we introduce an EAO solution and demonstrate its effectiveness and superiority over classical algorithms such as AO, PSO, and GWO in finding the optimal solution. In the following section, we explain the classical AO and the proposed EAO algorithms.

III. Preliminaries

A. Aquila Optimizer (AO) Algorithm

The Aquila Optimizer (AO) algorithm, proposed by Abualigah et al. in 2021 [20], is a meta-heuristic approach that addresses various optimization problems. AO draws inspiration from the hunting and prey-catching behavior of the Aquila bird, incorporating four key strategies, as follows:

1) *Vertical Pursuit: The Aquila's Swift Dive Strategy*: This strategy involves a high-altitude flight to scan and search for potential targets, followed by a precise and rapid vertical dive towards the intended prey. Mathematically, this behavior can be represented as:

$$S'^{(I+1)} = S'^{I}_{best} \times \left(1 - \frac{I}{I_{max}}\right) + \left(S^I_m - S'^{I}_{best} \times rand\right), \tag{9}$$

where $S'^{(I+1)}$ represents the obtained solution, indicating the index of the selected active PD at iteration $I+1$. S'^{I}_{best} denotes the optimal selected PD index achieved at the I^{th} iteration. The variable $rand$ corresponds to a random number generated from a Gaussian distribution ranging from 0 to 1. I_{max} is the maximum number of iterations. S^I_m represents the average value of the obtained solutions during the current iteration I. It can be given by $S^I_{avg} = \frac{1}{Ns} \sum_{i=1}^{N_s} S'^{I}_{i}$, where N_s is the number of population size.

2) *Aquila's Precision Hover-Glide Maneuver*: In this strategy, the Aquila bird transitions from a high altitude flight to a hovering position directly above its prey's location, enabling precise and controlled glide attacks. The mathematical formulation for updating the solution based on this strategy can be expressed as:

$$S'^{(I+1)} = S'^{I}_{best} \times LV(D_{im}) + S'^{I}_{R} + (b-a) \times rand, \tag{10}$$

where D_{im} represents the dimensionality of the problem. S'^{I}_{R} denotes the randomly selected index of the active PD, a and b are the search shape, and LV represents the Levy flight distribution function.

3) *Targeted Descent: The Aquila's Precision Approach*: The Aquila bird first locates the general position of its prey and then makes a gradual vertical descent towards the target. The preliminary attack associated with this strategy can be formulated as follows:

$$\begin{aligned} S'^{(I+1)} = & \left(S'^{I}_{best} - S^I_m\right) \times \alpha - rand \\ & + ((UB - LB) \times rand + LB) \times \delta, \end{aligned} \tag{11}$$

where δ and α are the exploitation adjustment parameters set to 0.1. Additionally, LB and UB represent the lower and upper bounds, respectively.

4) *Ground Tracer: The Aquila's Precision Pursuit*: In this strategy, the Aquila bird descends to the ground to trace the escape path of its prey and attempts to snatch it. Finally, the bird attacks the prey at its last known location. This pattern can be expressed as:

$$\begin{aligned} S'^{(I+1)} = & Q \times S'^{I}_{best} - \left(A_1 \times S'^{t} \times rand\right) \\ & - A_2 \times LV(D_{im}) + rand \times A_1 \end{aligned}, \tag{12}$$

where A_1 represents the random motion parameter associated with the bird's tracking process, which is calculated as $A_1 = 2 \times \text{rand} - 1$. Q is the quality function used for balancing search strategies, and is defined as $Q = I^{\frac{2 \times \text{rand} - 1}{(1 - I_{\text{max}})^2}}$. Also, A_2 corresponds to the flight slope adopted by the Aquila to pursue the target, and it can be expressed as $A_2 = 2 \times \left(1 - \frac{I}{I_{\text{max}}}\right)$.

B. Fitness Distance Balance (FDB)

The FDB selection method, introduced by Kahraman et al. [21], was designed to improve the search performance of meta-heuristic algorithms by identifying robust individuals based on their traits. These individuals have a significant impact on shaping the future population and effectively guiding the search process. The method utilizes a scoring system that evaluates potential solutions using their fitness values and proximity to the population's best solution. This ensures the prioritization of high fitness candidates while avoiding solutions that closely approach the optimum. The primary steps of the FDB method can be summarized as follows:

For a population P with N variables and M candidate solutions, the fitness values FV of these solutions are obtained through the objective function. Thus, we can represent the population vectors P and their corresponding fitness values as follows:

$$P \equiv \begin{bmatrix} S'_{11} & \cdots & S'_{1M} \\ \vdots & \ddots & \vdots \\ S'_{N1} & \cdots & S'_{NM} \end{bmatrix}, FV \equiv \begin{bmatrix} f_1 \\ \vdots \\ f_N \end{bmatrix}. \tag{13}$$

Let S'_{best} represent the best solution within the population P. The Euclidean distance between the i^{th} solution candidate S'_i and the best solution S'_{best} can be calculated using the following formula:

$$D_{S_i} = \sqrt{\left(S'_{1[i]} - S'_{1[\text{best}]}\right)^2 + \left(S'_{2[i]} - S'_{2[\text{best}]}\right)^2 + \cdots + \left(S'_{M[i]} - S'_{M[\text{best}]}\right)^2} \tag{14}$$

The distance vector D_S $(N \times 1)$ for the population P can be represented as $D_S \equiv [d_1 \ \cdot \ \cdot \ d_N]^T$.

Based on provided fitness values in equation (13) and the calculated distance from equation (14), the FDB score can be expressed as follows:

$$\forall_{i=1}^{N} S_i, \quad C_{S_i} = \Omega * \text{norm}FV_i + (1 - \Omega) * \text{norm}D_{S_i}, \tag{15}$$

where Ω is the weighting coefficient, normFV_i and normD_{S_i} denote the normalized fitness and distance values, respectively.

Finally, the N-dimensional vector C_S $(N \times 1)$ is obtained, which represents the FDB scores of individuals in the population P. It is given by $C_S \equiv [c_1 \ \cdot \ \cdot \ c_N]^T$.

IV. Proposed EAO Algorithm Structure

In this section, we provide a detailed description of the structure of our proposed EAO algorithm. The central idea behind the EAO algorithm is to enhance the optimization performance of the original AO algorithm by integrating FDB selection method. This strategy enables the efficient selection of reference positions to guide the AO search process. This maintains a diverse set of followers and prevents the algorithm from getting trapped in local optima. In our research, we employ the FDB method to guide the search in both Aquila's swift dive and targeted descent precision strategies.

$$S^{(I+1)} = FDB^I \times \left(1 - \frac{I}{I_{max}}\right) + \left(S_m^I - FDB^I \times rand\right), \tag{16}$$

$$\begin{aligned} S^{(I+1)} = &\left(FDB^I - S_m^I\right) \times \alpha - rand \\ &+ ((UB - LB) \times rand + LB) \times \delta \end{aligned} \tag{17}$$

Here, FDB^I represents the population leader generated through the FDB selection method. All steps of the proposed EAO method are described in Algorithm 1.

Algorithm 1 The pseudo-code of the EAO Algorithm

Initialize the population and the parameters of Aquila individuals $S'_i (i = 1, 2, ..., N_s)$
while $I \leq I_{max}$ **do**
  Compute the objective function values of each Aquila $f(S'_i)$
  Determinate the best solution obtained S'_{best}
  for $i = 1, 2, ..., N_s$ **do**
    Update the mean value of the current solution S_m.
    Update $LV(D_{im}), a, b, Q, A_1, A_2$, etc.
    if $I \leq \frac{2}{3} \times I_{max}$ **then**
      if $rand \leq 0.5$ **then**
        Update the current solution S'_i using (16)
      else
        Update the current solution S'_i using (10)
      end if
    else
      if $rand \leq 0.5$ **then**
        Update the current solution S'_i using (17)
      else
        Update the current solution S'_i using (12)
      end if
    end if
    if $f({S'_i}^{(t+1)}) > f({S'_i}^{t})$ **then**
      ${S'_i}^{t} = {S'_i}^{(t+1)}$
      if $f({S'_i}^{(t+1)}) > f({S'}^{t}_{ibest})$ **then**
        ${S'}^{t}_{ibest} = {S'_i}^{(t+1)}$
      end if
    end if
  end for
  I=I+1
end while
Return the best solution S'_{ibest}

V. Performance Results and Discussions

A. Numerical Parameters

For simulation analysis, we consider a room with dimensions of 10×10×3, where L = 9, M = 5, ρ = 0.54 A/W, and D_r = 1 cm. Additionally, we assume P_t = 11 W, N_0 = 10^{-21}A^2/Hz, B = 1 MHz, and $P_{e_{\text{th}}}$ = 10^{-6}. Furthermore, we consider $\mathcal{Q}$ = 2, w_1 = 0.7, and w_2 = 0.3. We investigate different user numbers, including N = 20, 30, 40, and 50. Our simulations are performed in MATLAB software, utilizing 1000 iterations and an average of 30 executions to minimize the effects of randomness and obtain reliable results.

B. Simulation Results and Discussions

In the following, we investigate the impact of varying user distributions and user numbers on the performance of our proposed approach in terms of capacity and fairness.

We investigate the effect of varying the distribution and the number of users on the performance of our proposed approach in terms of capacity and fairness. To accomplish this, we conduct a comparative study with AO, PSO, and GWO algorithms to demonstrate the efficacy of our proposed approach. Specifically, our proposed approach is evaluated in three realistic scenarios, including:

TABLE I. Capacity and Fairness for stationary scenario (i.e., Scenario 1)

	EAO	AO	PSO	GWO
Capacity (Mbit/s)	**448**	446	420	444
Fairness	**0.998**	0.997	0.994	0.997

TABLE II. Capacity and Fairness for moving scenario (i.e., Scenario 2)

	Scenarios	EAO	AO	PSO	GWO
Capacity (Mbit/s)	Sc1	**296**	294	282	293
	Sc2	**295.9**	294	279	294
	Sc3	**294.8**	293	281	293
Fairness	Sc1	**0.998**	0.997	0.995	0.997
	Sc2	**0.999**	0.998	0.995	0.998
	Sc3	**0.998**	0.997	0.993	0.997

a) ***Scenario 1****: Stationary Users:* In this scenario, all users are stationary in a defined area. We consider N_1 = 30 users and analyze the performance of our approach in terms of capacity and fairness. Table I shows the capacity and fairness results for all considered algorithms. It is observed that the EAO algorithm outperformed other algorithms in both the capacity and fairness, achieving significantly higher performance levels. For instance, consider EAO algorithm, the achieved capacity is 448 Mbit/s with an improvement of 2 Mbit/s, 28 Mbit/s, and 3 Mbit/s compared to AO, PSO, and GWO, respectively. It can be also observed that our proposed EAO scheme achieves higher bit-rate fairness compared to other algorithms. Numerically, the EAO algorithm achieves a fairness index of 0.998, while the values for AO, PSO, and GWO algorithms are 0.997, 0.994, and 0.997, respectively (i.e., see Table I).

b) ***Scenario 2****: Moving Users:* In this scenario, all users move in a predefined pattern at time t denoted by Sc1, Sc2, and Sc3. We consider N_2 = 20 users and we evaluate the performance of our approach compared to other state-of-the art algorithms. Table II presents the capacity and fairness for all considered algorithms. The results show that the EAO algorithm exhibits superior performance compared to other algorithms across all tested scenarios. For instance, in Sc1, EAO achieves a capacity of 296 Mbit/s, which is 2 Mbit/s, 14 Mbit/s, and 3 Mbit/s higher than AO, PSO, and GWO, respectively. Similarly, for Sc3, the obtained fairness values are 0.998, 0.997, 0.993, and 0.997 for EAO, AO, PSO, and GWO algorithms, respectively.

c) ***Scenario 3****: Random Users:* In this scenario, we assume that all users are randomly distributed, and we evaluate the performance of the proposed algorithm on a large scale by varying the number of users from 20 to 50. Our evaluation will focus on two key metrics: capacity and fairness. Table III displays the capacity under various numbers of users. Notably, the EAO algorithm has demonstrated higher capacity than other algorithms. For example, when considering N_3 = 20 users and the EAO algorithm, a capacity of 295.5 Mbit/s is achieved, with an improvement of 1.5 Mbit/s, 12.7 Mbit/s, and 0.8 Mbit/s compared to AO, PSO, and GWO algorithms, respectively. Additionally, we present fairness at different number of users in Table III. The results show that the proposed EAO algorithm consistently outperforms the other algorithms across different numbers of users. For instance, when considering N_3 = 50 users, the fairness index achieved by the EAO algorithm is 0.998, while it reduces to 0.997, 0.996, and 0.997 for AO, PSO, and GWO algorithms, respectively.

TABLE III. Capacity and Fairness for random scenario (i.e., Scenario 3)

	N	EAO	AO	PSO	GWO
Capacity (Mbit/s)	20	**295.5**	294	282.8	294.7
	30	**450.3**	441.3	415.1	438.1
	40	**596.1**	587.4	554.7	587.3
	50	**736**	728.7	702.1	734
Fairness	20	**0.998**	0.998	0.996	0.997
	30	**0.999**	0.998	0.996	0.998
	40	**0.998**	0.997	0.997	0.998
	50	**0.998**	0.997	0.996	0.997

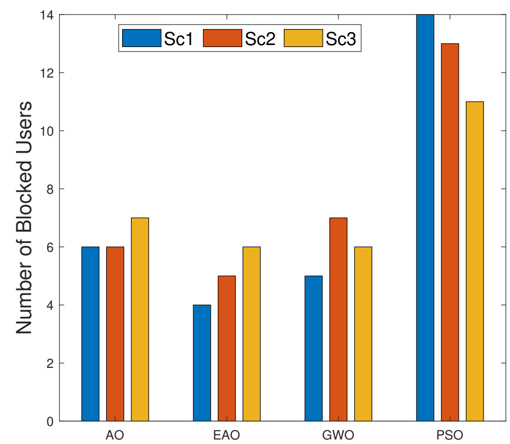

Fig. 3: Number of blocked users for different algorithms considering $P_{e_{th}} \leq 10^{-6}$.

In Fig. 3, we present the results for the number of blocked users with the proposed EAO scheme and other benchmark schemes assuming a BER threshold of $P_{e_{th}} = 10^{-6}$. The results reveal that the proposed EAO scheme demonstrates superior performance compared to other schemes by effectively minimizing the number of unserved users in all three scenarios (Sc1, Sc2, and Sc3). For instance, in Sc1, the proposed EAO scheme has only 4 blocked users, whereas GWO has 5, AO has 6, and PSO has a significantly higher number of blocked users at 14.

C. Convergence Analysis

Fig. 4 illustrates a comparison of the obtained best solutions across iterations for all algorithms considered. Our analysis reveals that the number of required iterations depends significantly on the target achieved capacity. For instance, when aiming for a capacity of 3.38 Mbit/s, the optimal number of iterations is approximately 10. However, as the target capacity

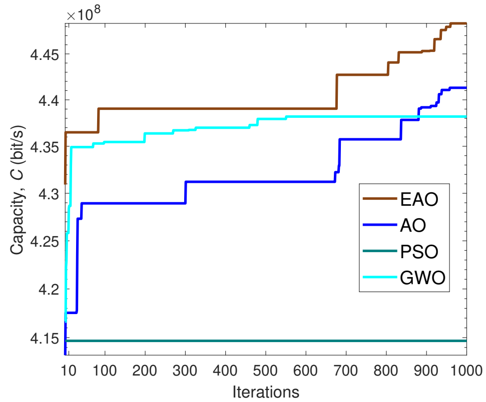

(a)

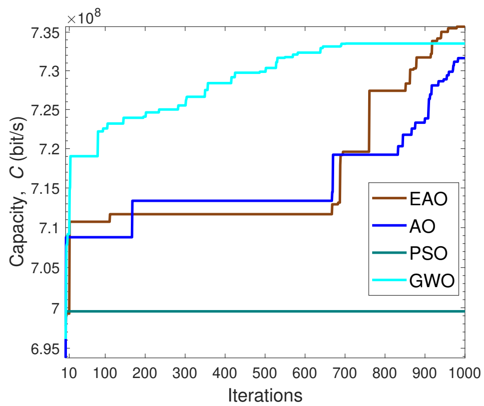

(b)

Fig. 4: Convergence analysis assuming scenario 3 (a) 30 users (b) 50 users

increases to 4.4 Mbit/s, the number of iterations sharply rises to around 680. Furthermore, when targeting a capacity of 4.48 Mbit/s, the number of iterations further increases to about 940. Notably, Fig. 4 also demonstrates that the proposed Enhanced EAO algorithm outperforms other algorithms in terms of convergence efficiency. Specifically, EAO achieves superior convergence compared to both GWO, which shows no further improvement after iteration 550 (see Fig. 4(a)), and PSO, which becomes trapped in a single optimum from the very first iteration. Furthermore, when comparing EAO with the original AO, it is evident that EAO achieves maximum capacity with significantly fewer iterations. For instance, when aiming to achieve a capacity of 7.35 Mbit/s, EAO required 970 iterations, whereas the original AO needed 995 iterations.

VI. Conclusion

This paper introduced the Enhanced Aquila Optimizer (EAO), an efficient optimization scheme for resource allocation in indoor multi-user IoT-VLC systems. The proposed algorithm is designed to maximize system capacity, ensure fairness, and reliable communication among users, while minimizing power consumption at the receiver side. To achieve these objectives, we integrated a Fitness Distance Balance selection method into the AO algorithm to improve its performance. Through extensive simulations, we demonstrated the superior performance of the EAO algorithm in finding optimal solutions compared to classical AO and other state-of-the-art algorithms in various scenarios and settings. In summary, the proposed EAO algorithm makes a noteworthy contribution to the field of indoor multi-user IoT-VLC systems. It offers a promising solution for optimizing resource allocation and enhancing system performance. It is worth noting that our current work focused on a fixed orientation of the PD receivers. However, as part of our future work, we intend to investigate the effects of random orientation and direction of the PDs, which will enhance the algorithm's adaptability and practicality in real-world VLC systems.

VII. Acknowledgment

The authors want to thank the supports from UiT - The Arctic University of Norway and EU Interreg Aurora program via funding the project HE4T - Harvesting Energy for Data Acquisition and Transfer and this work.

References

[1] L. Chettri and R. Bera, "A comprehensive survey on internet of things (IoT) toward 5G wireless systems," *IEEE Internet of Things J.*, vol. 7, no. 1, pp. 16–32, Jan. 2020.

[2] G. A. Akpakwu *et al.*, "A survey on 5G networks for the internet of things: Communication technologies and challenges," *IEEE Access*, vol. 6, pp. 3619–3647, Jan. 2018.

[3] A. Al-Fuqaha *et al.*, "Internet of things: A survey on enabling technologies, protocols, and applications," *IEEE Commun. Surveys Tuts.*, vol. 17, no. 4, pp. 2347–2376, June 2015.

[4] T. Besjedica, K. Fertalj, V. Lipovac, and I. Zakarija, "Evolution of hybrid LiFi–WiFi networks: A survey," *Sensors*, vol. 23, no. 9, p. 4252, 2023.

[5] H. Zhou *et al.*, "Design and implementation of wireless optical access system for VLC-IoT networks," *J. Lightw. Technol.*, vol. 41, no. 8, pp. 2369–2380, April 2023.

[6] I. Demirkol *et al.*, "Powering the internet of things through light communication," *IEEE Commun. Mag.*, vol. 57, no. 6, pp. 107–113, June 2019.

[7] M. W. Eltokhey *et al.*, "Optimization of receivers' field of views in multi-user vlc networks: A bio-inspired approach," *IEEE Wirel. Commun.*, vol. 29, no. 2, pp. 132–139, April 2022.

[8] M. Obeed *et al.*, "On optimizing VLC networks for downlink multi-user transmission: A survey," *IEEE Commun. Surveys Tuts.*, vol. 21, no. 3, pp. 2947–2976, March 2019.

[9] H. Yang *et al.*, "Coordinated resource allocation-based integrated visible light communication and positioning systems for indoor IoT," *IEEE Trans. Wireless. Commun.*, vol. 19, no. 7, pp. 4671–4684, July 2020.

[10] S. Chang *et al.*, "Indoor visible light communication scheduling for IoT scenarios with short blocklength," in *2020 IEEE/CIC International Conference on Communications in China (ICCC Workshops)*. IEEE, 2020, pp. 185–190.

[11] H. B. Eldeeb *et al.*, "Optimal resource allocation and interference management for multi-user uplink light communication systems with angular diversity technology," *IEEE Access*, vol. 8, pp. 203 224–203 236, Nov. 2020.

[12] S. I. Mushfique *et al.*, "Resource optimization in visible light communication for internet of things," in *2019 IEEE International Symposium on Local and Metropolitan Area Networks (LANMAN)*. IEEE, 2019, pp. 1–6.

[13] M. Uysal *et al.*, "IEEE 802.15.7r1 reference channel models for visible light communications," *IEEE Commun. Mag.*, vol. 55, no. 1, pp. 212–217, Jan. 2017.

[14] S. Yahia *et al.*, "Enhancement of vehicular visible light communication using spherical detector and custom lens combinations," *IEEE Access*, vol. 11, pp. 21 600–21 611, Feb. 2023.

[15] Z. Chen, D. Tsonev, and H. Haas, "Improving SINR in indoor cellular visible light communication networks," in *2014 IEEE Int. Conf. Commun. (ICC)*. IEEE, 2014, pp. 3383–3388.

[16] I. The MathWorks, *VLC CIR Toolbox*, Natick, Massachusetts, United State, 2019. [Online]. Available: https://www.mathworks.com/help/symbolic/

[17] Z. Wang, Q. Wang, W. Huang, and Z. Xu, *Visible light communications: Modulation and signal processing*. John Wiley & Sons, 2017.

[18] E. Björnson *et al.*, "Intelligent reflecting surface versus decode-and-forward: How large surfaces are needed to beat relaying?" *IEEE Wireless Commun. Lett.*, vol. 9, no. 2, pp. 244–248, Feb 2020.

[19] Y. S. Eroglu *et al.*, "Multi-element transmitter design and performance evaluation for visible light communication," in *2015 IEEE Globecom Workshops (GC Wkshps)*. IEEE, 2015, pp. 1–6.

[20] L. Abualigah *et al.*, "Aquila optimizer: A novel meta-heuristic optimization algorithm," *Comput. Ind. Eng.*, vol. 157, p. 107250, July 2021.

[21] H. T. Kahraman *et al.*, "Fitness-distance balance (FDB): a new selection method for meta-heuristic search algorithms," *Knowl Based Syst.*, vol. 190, p. 105169, Feb. 2020.